

Received January 30, 2019, accepted February 25, 2019, date of publication February 28, 2019, date of current version March 18, 2019.

Digital Object Identifier 10.1109/ACCESS.2019.2902127

# Optimal Estimation and Fundamental Limits for Target Localization Using IMU/TOA Fusion Method

**CHENG XU<sup>1</sup>, (Member, IEEE), JIE HE, YUANYUAN LI,**

**XIAOTONG ZHANG<sup>1</sup>, (Senior Member, IEEE),**

**XINGHANG ZHOU, AND SHIHONG DUAN**

School of Computer and Communication Engineering, University of Science and Technology Beijing, Beijing 100083, China

Beijing Advanced Innovation Center for Materials Genome Engineering, University of Science and Technology Beijing, Beijing 100083, China

Beijing Key Laboratory of Knowledge Engineering for Materials Science, Beijing 100083, China

Corresponding authors: Jie He (hejie@ustb.edu.cn) and Xiaotong Zhang (zxt@ies.ustb.edu.cn)

This work was supported in part by the National Key R&D Program of China under Grant 2016YFC0901303, in part by the National Natural Science Foundation of China under Project 61671056, Project 61302065, Project 61304257, and Project 61402033, in part by the Beijing Natural Science Foundation under Project 4152036, and in part by the Tianjin Special Program for Science and Technology under Grant 16ZXCXSF00150.

**ABSTRACT** Localization is one of the most important topics of the cyber-physical system. In the last decades, much attention has been paid to the precise localization and performance evaluation in wireless sensor networks. The inertial measurement unit (IMU) and time-of-arrival (TOA) fusion is a state-of-the-art method to solve the accumulative error and drifting problem faced by the sole IMU positioning and navigation method. Many of the existing studies are based on optimization. However, they usually face problems of non-convexity of the objective function, falling into local optimum, and the requirements for the prior/posterior probability distribution of measured values. All these reasons limit its practical applications toward accurate target tracking. This paper presents a Chebyshev-center-based optimization method. Geometrically considering the real position of the target, it aims at improving the target tracking accuracy. Cramér–Rao lower bound (CRLB) and posterior CRLB for IMU/TOA fusion are derived to characterize both the spatial and temporal localization performance of the proposed fusion method. The simulation results show that the proposed fusion method in this paper has obvious spatial–temporal performance advantages in theory. Practical use cases are also conducted, and the experimental results show that the proposed method significantly decreases the drift errors and has a lower tracking error compared with the state of the art.

**INDEX TERMS** Inertial measurement unit (IMU), time of arrival (TOA), Cramér–Rao lower bound (CRLB), posterior Cramér–Rao lower bound (PCRLB), optimization, target tracking.

## I. INTRODUCTION

Localization is one of the most important topics of cyber-physical system (CPS) [1]. The acquisition of target location information is particularly important in the applications of wireless sensor networks (WSNs), such as military deployment [2], security monitoring [3], and intelligent medical care [4]. Location-based services are inseparable parts of social development, greatly facilitating people's daily lives [5], [6].

The associate editor coordinating the review of this manuscript and approving it for publication was Valerio Freschi.

Global Positioning System (GPS) is an all-around, all-weather, full-time, high-precision satellite navigation system that provides global users with low-cost, high-precision navigation information [7]. However, GPS is limited in harsh environments, such as indoor and high building compact districts, where GPS signals cannot penetrate most of the obstacles [8]. Inertial navigation technology [2] stands out in these conditions, where the usage of GPS is restricted, with use of inertial measurement units (IMUs). However, INS is not suitable for longterm tracking applications and difficult to get practical promotion, because of accumulative errors and drifting problem [2], [3]. In order to solve this issue, existing

literatures generally adopt multi-source fusion approaches. Time of Arrival (TOA) enhanced fusion method [4] has been used in many applications, due to its low cost, high precision and easy deployment advantages [5], [6], [9].

Fusion filtering methods, such as Kalman [10] and particle filtering [12], are widely used in IMU/TOA fusion-based localization applications. Zhao *et al.* [10] proposed a Kalman/UFIR filtering method for state estimation with uncertain parameters and noise statistics. Briese *et al.* [11] presented an adapting covariance Kalman filter based on the fusion of Ultra-Wideband (UWB) and inertial measurements. Since both sensor results were separately used in the Kalman filter, no registration between the implemented sensors was needed. Kim *et al.* [12] proposed a fusion algorithm based on a particle filter using vertical and road intensity information for robust vehicle localization in a large scale urban area. However, filtering methods lack in terms of dynamic behavior and the algorithm performance varies with the change of state matrix [11], [12]. They can to some extent slow down the error accumulation process, but not eliminate it completely [20], [34]. With the booming of artificial intelligence, deep neural networks [13] have been applied in the fusion of multi-sensors, while the requirement of a large scale of data still remains a big challenge in practical applications.

In addition to filtering methods, the estimation of target position is generally regarded as an optimization problem [1], in order to keep highly consistent between the position estimation result and distance measurements. Mieza *et al.* [14] utilized Maximum Likelihood Estimation (MLE) to obtain an estimation result of the target position by maximizing the likelihood function of the target position. However, its accuracy is related to the statistical accuracy of measurement errors, and often introduces large positioning errors in practical use cases [15], [16]. Besides, MLE are often non-convex [17]. In the optimization process, gradient descent searching algorithm also needs a reasonable initial value to complete the global search [18], [19]. Otherwise, it is easy to fall into the local optimum and cannot get the ideal solution. In order to solve this problem, Zhang *et al.* [21] adopted the method of semi-positive definite relaxation (SDR) to relax the non-convex problem into a convex problem, and then solve it by convex programming method.

The least square (LS) algorithm [22], [23] is also a commonly used optimization method. Compared with MLE, LS does not require a priori statistical information of the measured values. Both MLE and LS are non-Bayesian estimates, which are the same when the measurement error is a Gaussian distribution of zero-mean [22]. Optimization algorithms based on maximum posteriori probability (MAP) [24], [25] are also used in localization algorithms. However, although it to some extent solves the GDOP (Geometric Dilution of Precision) dependence problem with use of topological geometric localization algorithm [26], the posterior probability distribution of the measured parameters is often difficult to be obtained accurately, which also limits the application of MLE and LS [22].

Existing studies usually regard the location estimation of targets as a global optimization problem based on loss function, such as [1] and [14]. Since the true positions of targets are not known, the loss function is generally defined to minimize the overall mean square errors (MSEs) between measurements and potential solutions. Then the problem arises. The overall MSE may be ideal, but the positioning results of some nodes may be of high accuracy, whereas the errors of some nodes are particularly larger. Thus, it is not reasonable to define the objective function as “minimized positioning error” [1], [14], [19].

Above all, although many related researches have been done, IMU/TOA fusion methods still have lots of room for improvement to achieve better tracking accuracy in various CPS applications. Besides, the localization results of target nodes are uncertain due to the influence of random factors, such as noise, fading, multipath, and non-line-of-sight propagation [11], [30]. Thus, how to evaluate the performance of localization algorithms accurately is also one of the most important problems in CPS. Cramér-Rao lower bound (CRLB) [31] defines the theoretical lower bound of the unbiased estimator variance, and it is generally used as a criterion for evaluating the performance of a positioning system [32], [33]. However, CRLB only focuses on the influence of the relationship between relative positions in spatial state on the accuracy of the positioning target, neglects the time information, and cannot meet the requirements of temporal evaluation in the positioning system. The posterior Cramér-Rao lower bound (PCRLB) [35], [36] considers the time domain information and can be used as another criterion for the performance evaluation of the positioning system.

Based on above analysis, in this paper, focusing on the concept of Chebyshev-center [37] in topological geometry, we propose an objective function construction method considering the real position of target nodes. We define the objective function as “minimizing the error of the worst case in the feasible domain”(worst-case error), which is more in line with practice and our common sense. The main contributions of this paper are as follows:

- A Chebyshev-center-based optimization method is proposed to fuse IMU and TOA information for target localization applications in CPS. The proposed method can to a large extent compensate the error accumulation problem of IMU, and is obviously superior to state-of-the-art methods.
- The real position of the target is introduced into the objective function, in order to solve the non-convex optimization problem based on the concept of Chebyshev-center. We define the objective function as “minimizing the error of the worst case in the feasible domain”(worst-case error), which is more in line with practice and our common sense.
- Comprehensively, we verified the effectiveness of proposed method in theory and practice. By deducing the CRLB and PCRLB of IMU/TOA fusion system, we theoretically prove the feasibility and optimal performance

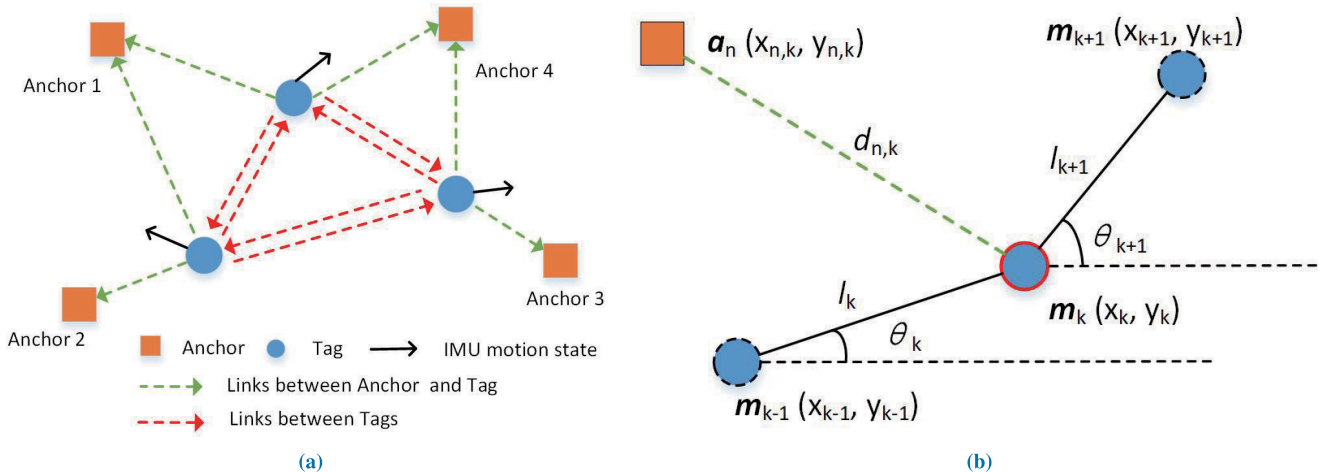


**FIGURE 1.** Schematic diagram of multi-targets' cooperative localization in 2D scenarios. (a) Nodes and parameters definition. (b) The state transition of the target node.

of proposed method in both spatial and temporal aspects. Practical use cases for 2D navigation robots and 3D human motion tracking applications are carried out to verify the performance of proposed method when compared with state-of-the-arts.

The remainder of the paper is organized as follows. Section II gives the problem formulation and error modeling of systems. Section III presents the proposed optimal estimation method. Section IV illustrates both spatial and temporal performance evaluation methods and verifies the performance of proposed method theoretically. Practical use cases are presented in Section V. Conclusions are drawn in Section VI.

## II. PROBLEM FORMULATION AND ERROR MODELING

### A. PROBLEM DESCRIPTION

To simplify the discussion of the problem, we mainly describe multi-targets' cooperative localization in 2D scenarios in this section. Models in 3D conditions can be easily extended. As indicated in Fig. 1-(a), nodes with known and fixed coordinates are defined as reference nodes (i.e., Anchors), and nodes with unknown coordinates are defined as mobile nodes (i.e., Tags). The relative distance between the nodes can be obtained by TOA ranging.

Define a set  $P_t = \{1, 2, \dots, N\}$  with  $N$  mobile targets whose position is unknown, where measured coordinate of the  $i$ th moving target at time  $k$  is  $m_{i,k} = [x_{i,k}, y_{i,k}]$ . For convenience, in the general description that follows, we usually neglect the id indexes of potential targets.

Define a set  $P_a = \{N+1, \dots, N+M\}$  with  $M$  reference base stations, where the coordinate of the  $j$ th reference base station is represented as  $a_j = [x_j, y_j]$ .

Spatially due to the limitation of communication capability between nodes, a certain mobile target can only communicate with some of mobile targets or reference base stations within a certain range around it. Therefore, we define variables  $L_a$  and

$L_t$  to respectively represent the set of possible links between the moving targets and the anchors, and links between one moving target and the other. Correspondingly, the interconnected moving target and the anchor set are represented as  $N_a$  and  $N_t$  respectively. Then, the entire positioning network can be represented as a set with target nodes and links:  $\mathcal{G} = (N, L)$ .

In terms of temporal sequence, one target may move in a certain list of states, as shown in Fig. 1-(b). The state information matrix of the target node is  $m = [m_1, m_2, \dots, m_K]^T$  and  $K$  is the total state number. For each element in the state information matrix, the following formula can be obtained by

$$m_k = m_{k-1} + l_k w_k \quad (1)$$

where  $l_k$  is the moving step of the node from state  $k-1$  to state  $k$ ,  $w_k = [\cos\theta_k, \sin\theta_k]^T$  is the moving direction of the node.

### B. ERROR MODELING

The location of target nodes are uncertain because of the influence of random factors, such as noise, fading, multipath, and non-line-of-sight propagation, which ultimately affects the positioning accuracy. Generally, in localization and navigation problems, the random walk model [27], [49], such as our model described in Fig. 1-(b), can be modeled as a Gauss-Markov process, whose parameters generally are composed of distance and angle information. Firstly, we model the possible errors in presented localization schematic.

The step size estimate based on the IMU can be expressed as

$$\hat{l}_k = l_k + u_k, u_k \sim N(\theta, \sigma_{1,k}^2) \quad (2)$$

where  $l_k$  is the actual step size, i.e.,

$$l_k = \sqrt{(x_k - x_{k-1})^2 + (y_k - y_{k-1})^2} \quad (3)$$

$u_k$  is the step error and obeys the Gaussian distribution with a mean of 0 and a covariance of  $\sigma_{1,k}^2$ .

The horizontal angle estimate based on the IMU can be expressed as

$$\hat{\theta}_k = \theta_k + \varepsilon_k, \quad \varepsilon_k \sim N(0, \sigma_{2,k}^2) \quad (4)$$

where  $\theta_k$  is the actual horizontal angle, i.e.,

$$\theta_k = \arctan \frac{y_k - y_{k-1}}{x_k - x_{k-1}} \quad (5)$$

$\varepsilon_k$  is the horizontal angle error and obeys the Gaussian distribution with a mean of 0 and a covariance of  $\sigma_{2,k}^2$ .

The distance between the target node and the anchor node measured by the TOA ranging method is estimated as

$$\hat{d}_{n,k} = \|\mathbf{m}_k - \mathbf{a}_n\|_2 + e_k = d_{n,k} + e_k \quad (6)$$

where  $d_{n,k}$  is the actual distance between the target node and the  $n$ th anchor node, i.e.,

$$d_{n,k} = \sqrt{(x_k - x_{n,k})^2 + (y_k - y_{n,k})^2} \quad (7)$$

where  $e_k$  is the ranging error caused by the TOA method and obeys a Gaussian distribution with a mean of 0 and a variance of  $\sigma_{3,k}^2$ , i.e.,  $e_k \sim N(0, \sigma_{3,k}^2)$ .

### III. OPTIMAL ESTIMATION FUSION METHOD

In optimization method, the estimated target position is obtained by optimizing the objective function under constraint conditions. Based on the concept of Chebyshev-center [37] in topological geometry, we propose an optimization method considering the real position of the target node, and solve the precise positioning problem by optimizing the solution of the worst positioning situation.

Under the condition that the IMU/TOA fusion system obtains the distance and angle parameters, we could 1) estimate the elliptical error by the IMU real-time tracking performance; 2) estimate the distance constraint error by TOA distance measurement; 3) estimated target location by the min-max optimization estimation method based on Chebyshev-center theory. Next, we will introduce the proposed IMU/TOA fusion-based optimization method from above mentioned aspects, namely elliptical error constraint, distance error constraint and optimization method.

#### A. ELLIPTICAL ERROR CONSTRAINT OF IMU

Measuring the uncertainty of points plays an important role in the research of multi-target tracking. It not only provides reasonable evaluation indicators for the effectiveness of positioning methods, but also provides a reference for how to further improve tracking accuracy.

In the error theory, the error ellipse plays an important role. At present, when studying the precision and uncertainty of point, the accuracy of plane point position often adopts error ellipse [38], [39] to visualize abstract point quality with intuitive 2D graphics and have many applications.

The error bound estimation of IMU can be represented by error ellipse. The direction of the long and short half axes of

the error ellipse represents the maximum and minimum error direction respectively; the size shows the standard deviation of the plane point error along the half-axis direction [39].

**Definition 1:** The point  $\mathbf{x} = (x, y)^T$  in the 2D IMU plane obeys the overall distribution  $N(\mu, \mathbf{B})$ , where  $\mu = (\mu_x, \mu_y)^T$ , the covariance matrix  $\mathbf{B} = \begin{bmatrix} \sigma_x^2 & \sigma_{xy} \\ \sigma_{yx} & \sigma_y^2 \end{bmatrix}$  is a second-order positive definite matrix,  $\sigma_x^2, \sigma_y^2$  are the variance of  $x, y$  respectively,  $\sigma_{xy}$  is covariance between variables.  $D = \{\mathbf{x} | (\mathbf{x} - \mu)^T \mathbf{B}^{-1} (\mathbf{x} - \mu) \leq R^2\}$  is defined as the error ellipse.

The joint probability density of a two-dimensional space point is expressed as:

$$f(x, y) = \frac{1}{(2\pi)\sqrt{|\mathbf{B}|}} \exp \left\{ -\frac{1}{2} (\mathbf{x} - \mu)^T \mathbf{B}^{-1} (\mathbf{x} - \mu) \right\} \quad (8)$$

It can be known from the positive definiteness of the covariance matrix  $\mathbf{B}$  that the characteristic values  $\lambda_1, \lambda_2$  of  $\mathbf{B}$  are both positive and there is an orthogonal matrix  $Q = (\vec{p}_1, \vec{p}_2)$ :

$$Q^T \mathbf{B} Q = \begin{bmatrix} \lambda_x & 0 \\ 0 & \lambda_y \end{bmatrix} \quad (9)$$

where  $\vec{p}_i$  is the eigenvector of  $\mathbf{B}$  corresponding to  $\lambda_i$ .

**Definition 2:**  $\mathbf{x}' = \mathbf{x} - \mu$ . The definition changes as follows:

$$\mathbf{x}' = (x', y')^T = Q(\bar{x}, \bar{y})^T = Q\bar{\mathbf{x}} \quad (10)$$

where,  $|J| = |\frac{\partial \mathbf{x}'}{\partial \bar{\mathbf{x}}} = |Q| = 1$ . Correspondingly, the error ellipse can be written as:

$$\begin{aligned} (\mathbf{x} - \mu)^T \mathbf{B}^{-1} (\mathbf{x} - \mu) &= \mathbf{x}'^T \mathbf{B}^{-1} \mathbf{x}' \\ &= \bar{\mathbf{x}}^T Q^T \mathbf{B}^{-1} Q \bar{\mathbf{x}} \\ &= \bar{\mathbf{x}}^T (Q^T \mathbf{B} Q)^{-1} \bar{\mathbf{x}} \leq R^2 \end{aligned} \quad (11)$$

which is  $\frac{\bar{x}^2}{\lambda_x} + \frac{\bar{y}^2}{\lambda_y} \leq R^2$ . The eigenvalues  $\lambda_x, \lambda_y$  are respectively the major and minor axis radius of the error ellipse.  $Q$  corresponds to the two-dimensional coordinate axis rotation matrix. Thus, the error constraint of IMU could be represented.

#### B. DISTANCE CONSTRAINT OF TOA

In a multi-target cooperative localization application, the relative distance between the nodes can be obtained by TOA ranging. Due to the difference in node type and target motion state, the distance relationship between nodes can be divided into the following categories:

##### 1) DETERMINISTIC DISTANCE CONSTRAINT

“Deterministic” refers that the reference node’s position is reliable, i.e., the measured value of the distance between Tag and Anchor, which is defined as:

$$\hat{d}_{ik} = d_{ik} + n_{ik} \quad (12)$$

where,  $d_{ik} = \|\mathbf{m}_i - \mathbf{a}_k\|$  is real distance between target  $i$  and base station  $k$ .  $|n_{ik}| \leq \gamma$ ,  $\gamma > 0$  is the error limit of ranging. According to the error estimate, the ranging value between

the moving target and the Anchor should satisfy the constraint interval:  $\underline{d}_{ik} \leq \widehat{d}_{ik} \leq \overline{d}_{ik}$ , where  $\underline{d}_{ik} = \widehat{d}_{ik} - \gamma$ ,  $\overline{d}_{ik} = \widehat{d}_{ik} + \gamma$ .

Distance measurement value between Anchor and Anchor: This type of distance does not change if the Anchor position is determined. The measurement has meaning when the anchor position is uncertain. This paper does not consider the uncertainty of the anchor position.

## 2) UNCERTAIN DISTANCE CONSTRAINTS

“Uncertain” refers that the reference node’s position is unreliable, i.e., the measured value between moving targets, which may be defined as:

$$\widehat{d}_{ij} = d_{ij} + n_{ij} \quad (13)$$

where,  $d_{ij} = \|\mathbf{m}_i - \mathbf{m}_j\|$  is real distance between target  $i$  and target  $j$ .  $|n_{ij}| \leq \gamma$ ,  $\gamma > 0$  is the error limit of ranging. According to the error estimate, the ranging value between the moving targets should satisfy the constraint interval:  $\underline{d}_{ij} \leq \widehat{d}_{ij} \leq \overline{d}_{ij}$ ,  $\underline{d}_{ij} = \widehat{d}_{ij} - \gamma$ ,  $\overline{d}_{ij} = \widehat{d}_{ij} + \gamma$ .

## 3) DISTANCE CONSTRAINT CONDITION

Considering the above two constraints, it should satisfy the following constraints for a given Tag:

$$\begin{aligned} \mathcal{C} = \{\mathbf{m}_i : \underline{d}_{ij} \leq \|\mathbf{m}_i - \mathbf{m}_j\| \leq \overline{d}_{ij}, \forall (i, j) \in L_t \\ \underline{d}_{ik} \leq \|\mathbf{m}_i - \mathbf{m}_k\| \leq \overline{d}_{ik}, \forall (i, k) \in L_a\} \end{aligned} \quad (14)$$

Optimization process is to solve the optimal solution satisfying the objective function in the feasible domain. We will detail the process of establishing the objective function in the next section.

## C. CHEBYSHEV CENTER BASED OPTIMIZATION METHOD

Based on above analysis, existing optimization objective functions have problems such as non-convex, GDOP insensitivity, and easily falling into local optimum. Therefore, it is necessary to design a reasonable objective function. In this section, we propose an objective function construction method considering the real position of target nodes, and optimizes the solution process by constructing a convex function. Since the real coordinates of the target node are introduced into the optimization function as an intermediate variable, GDOP information is also introduced therein.

Since the real target position is unknown, it is not reasonable to define the objective function as “minimized positioning error” [1], [41]. Therefore, we define the objective function as “minimizing the error of the worst case in the feasible domain”(worst-case error).

## 1) DEFINITION OF THE OBJECTIVE FUNCTION

*Definition 3:* the real locations are expressed as  $\mathbf{x} = [\mathbf{x}_1, \mathbf{x}_2, \dots, \mathbf{x}_N]^T \in R^{2N}$ , the target positions in the feasible domain are represented as  $\mathbf{m} = [\mathbf{m}_1, \mathbf{m}_2, \dots, \mathbf{m}_N]^T \in R^{2N}$ , and the target estimation positions in the feasible domain are represented as  $\hat{\mathbf{x}} = [\hat{\mathbf{x}}_1, \hat{\mathbf{x}}_2, \dots, \hat{\mathbf{x}}_N]^T \in R^{2N}$ .

Therefore, we define the position of the moving target  $i$  as  $\hat{\mathbf{x}}_i$ , then the worst case estimation error (worst-case) can be expressed as:

$$\max_{\mathbf{m}_i} \sum_{i=1}^N \|\mathbf{m}_i - \hat{\mathbf{x}}_i\|^2 \quad (15)$$

That is, to find the worst case estimation error of appropriate position in the feasible domain. We intend to find the optimal value, to minimize the worst case position estimation error of the above formula, namely

$$\begin{aligned} \min_{\hat{\mathbf{x}}} \max_{\mathbf{m} \in \mathcal{C}} Tr((\mathbf{m} - \hat{\mathbf{x}})(\mathbf{m} - \hat{\mathbf{x}})^T) \\ \text{s.t. } \frac{\overline{m}_{ix}^2}{\lambda_x} + \frac{\overline{m}_{iy}^2}{\lambda_y} \leq R^2 \quad (C1) \\ \underline{d}_{ij} \leq f_{ij}(\mathbf{m}) \leq \overline{d}_{ij}, \quad \forall (i, j) \in L_t \quad (C2) \\ \underline{d}_{ik} \leq f_{ik}(\mathbf{m}) \leq \overline{d}_{ik}, \quad \forall (i, k) \in L_a \quad (C3) \end{aligned} \quad (16)$$

where constraint (C1) is error ellipse constraint, (C2) and (C3) are deterministic and uncertainty constraints respectively.

$$\begin{aligned} f_{ij}(\mathbf{m}) = \mathbf{e}_{(2i-1)(2j-1)}^T \mathbf{m} \mathbf{m}^T \mathbf{e}_{(2i-1)(2j-1)}^T \\ + \mathbf{e}_{(2i)(2j)}^T \mathbf{m} \mathbf{m}^T \mathbf{e}_{(2i)(2j)}^T \end{aligned} \quad (17)$$

$$\begin{aligned} f_{ik}(\mathbf{m}) = \mathbf{a}_k \mathbf{a}_k^T - 2\mathbf{a}_{kx} \mathbf{m}^T \mathbf{e}_{2i-1} - 2\mathbf{a}_{ky} \mathbf{m}^T \mathbf{e}_{2i} \\ + \mathbf{e}_{2i-1}^T \mathbf{m} \mathbf{m}^T \mathbf{e}_{2i-1} + \mathbf{e}_{2i}^T \mathbf{m} \mathbf{m}^T \mathbf{e}_{2i} \end{aligned} \quad (18)$$

where  $\mathbf{e}_i \in R^{2n}$  is a column vector, the  $i$ th term is 1, and the remaining terms are 0;  $\mathbf{e}_{(i)(j)} \in R^2$  is a column vector, the  $i$ th term is 1, the  $j$ th term is -1, and the remaining terms are 0.

## 2) RELAXATION OF THE OBJECTIVE FUNCTION

Topological geometry regards above optimization as finding the Chebyshev-center in the feasible domain [37]. However, it is non-convex, so typical convex optimization algorithm cannot be directly used for solving the problem. Therefore, this paper draws on the relaxation method in the Chebyshev center problem, transforms (16) into convex optimization problem through relaxing the key variables condition, and simplifies the problem solving process.

Let  $\Delta = \mathbf{m} \mathbf{m}^T$ , then (16) becomes:

$$\min_{\hat{\mathbf{x}}} \max_{\mathbf{m} \in \mathcal{C}} Tr(\Delta - 2\hat{\mathbf{x}}\mathbf{m}^T + \hat{\mathbf{x}}\hat{\mathbf{x}}^T) \quad (19)$$

where  $\mathcal{G}$  is the updated feasible domain:

$$\begin{aligned} \mathcal{G} = \{(\mathbf{m}, \Delta) : \frac{\overline{m}_{ix}^2}{\lambda_x} + \frac{\overline{m}_{iy}^2}{\lambda_y} \leq R^2, \underline{d}_{ij} \leq g_{ij}(\Delta) \leq \overline{d}_{ij}, \forall (i, j) \\ \in L_t, \underline{d}_{ik} \leq g_{ik}(\mathbf{m}, \Delta) \leq \overline{d}_{ik}, \forall (i, k) \in L_a, \Delta = \mathbf{m} \mathbf{m}^T\} \end{aligned} \quad (20)$$

where

$$g_{ij}(\Delta) = \mathbf{e}_{(2i-1)(2j-1)}^T \Delta \mathbf{e}_{(2i-1)(2j-1)}^T + \mathbf{e}_{(2i)(2j)}^T \Delta \mathbf{e}_{(2i)(2j)}^T \quad (21)$$

$$\begin{aligned} g_{ik}(\mathbf{m}, \Delta) = \mathbf{a}_k \mathbf{a}_k^T - 2\mathbf{a}_{kx} \mathbf{m}^T \mathbf{e}_{2i-1} - 2\mathbf{a}_{km} \mathbf{m}^T \mathbf{e}_{2i} \\ + \mathbf{e}_{2i-1}^T \Delta \mathbf{e}_{2i-1} + \mathbf{e}_{2i}^T \Delta \mathbf{e}_{2i} \end{aligned} \quad (22)$$

where  $e_i \in R^{2n}$  denotes a column vector, the  $i$ th term is 1, and the remaining terms are 0;  $e_{(i)(j)} \in R^2$  denotes a column vector, the  $i$ th term is 1, the  $j$ th term is -1, and the remaining terms are 0.

The equality constraints  $\Delta = \mathbf{m}\mathbf{m}^T$  are not affine, which means the constraint set  $\mathcal{G}$  is a non-convex set [21]. In order to transform it to convex, we make the following relaxation:

$$\Delta \geq \mathbf{m}\mathbf{m}^T \quad (23)$$

As is well known, the above constraints can be written into:  $\begin{bmatrix} \Delta & \mathbf{m} \\ \mathbf{m}^T & 1 \end{bmatrix} \geq 0$ , that is, positive. The distance constraint can constitute a convex polyhedron, that is, it can also constitute a convex set.

Therefore, the objective function described in this paper is transformed into a convex optimization problem by slack variables:

$$\begin{aligned} \min_{\hat{\mathbf{x}}} \max_{(\mathbf{m}, \Delta) \in \mathcal{K}} & Tr(\Delta - 2\hat{\mathbf{x}}\mathbf{m}^T + \hat{\mathbf{x}}\hat{\mathbf{x}}^T) \\ \text{s.t. } & \frac{\bar{\mathbf{m}}_{ix}^2}{\lambda_x} + \frac{\bar{\mathbf{m}}_{iy}^2}{\lambda_y} \leq R^2 \\ & \underline{d}_{ij} \leq g_{ij}(\Delta) \leq \bar{d}_{ij}, \quad \forall (i, j) \in L_t \\ & \underline{d}_{ik} \leq g_{ik}(\mathbf{m}, \Delta) \leq \bar{d}_{ik}, \quad \forall (i, k) \in L_a \\ & \Delta \geq \mathbf{m}\mathbf{m}^T \end{aligned} \quad (24)$$

### 3) SOLUTION OF OBJECTIVE FUNCTION

Above mentioned objective function is a continuous, finite convex function. The outer layer of optimization function for minimizing is unconstrained, and the inner layer for maximizing is constrained. Since the feasible domains of the two layers for optimization are both non-empty closed convex sets, and the objective function is a linear function with  $\mathbf{m}$  and  $\Delta$ . It is continuous and finite on the set  $\mathbf{x} \times \mathcal{K}$ . From [21], we can exchange the order of inner and outer layer, which is

$$\max_{(\mathbf{m}, \Delta) \in \mathcal{K}} \min_{\hat{\mathbf{x}}} Tr(\Delta - 2\hat{\mathbf{x}}\mathbf{m}^T + \hat{\mathbf{x}}\hat{\mathbf{x}}^T) \quad (25)$$

Obviously, the optimal solution of the inner layer function is obtained at  $\hat{\mathbf{x}} = \mathbf{m}$ . Therefore, the above optimization function can be reduced to:

$$\max_{(\mathbf{m}, \Delta) \in \mathcal{K}} Tr(\Delta - \mathbf{m}\mathbf{m}^T) \quad (26)$$

### 4) GEOMETRICAL INTERPRETATION

The proposed method of minimizing the worst-case error, in terms of graphics, is to find the Chebyshev-center, which is the center of the smallest circumscribed circle that can wrap the polygonal area. Then, the formula (24) can be expressed geometrically as:

$$\begin{aligned} \mathbf{x}_{cheby} = \arg \min_{\hat{\mathbf{x}}} \max_{\mathbf{m} \in \mathcal{C}} & Tr((\mathbf{m} - \hat{\mathbf{x}})(\mathbf{m} - \hat{\mathbf{x}})^T) \\ \min_{\mathbf{x}_{cheby}} & \{r_{cheby} : \|\mathbf{m} - \mathbf{x}_{cheby}\| \leq r_{cheby}\} \end{aligned} \quad (27)$$

where,  $\mathbf{x}_{cheby}$  is of Chebyshev-center,  $r_{cheby}$  is the radius of the smallest circumscribed circle of the feasible domain corresponding to the Chebyshev-center. For non-convex feasible domains, the Chebyshev-center may appear outside the feasible domain, reducing the accuracy of the results. Therefore, we relaxed the feasible domain, that is, the Chebyshev-center after relaxation was selected as the optimal result.

The set within the Chebyshev circle is represented as:

$$\mathbf{m} = \mathbf{x}_{cheby} + \mu \quad (28)$$

where,  $\mu$  is 2D relaxation vector. Because the feasible domain is included in the Chebyshev circle:

$$\|\mu\| \leq r_{cheby} \quad (29)$$

Therefore, above formula satisfies the CVX [42] mechanism of problem solving.

## IV. THEORETICAL PERFORMANCE EVALUATION

In the above section, we present a Chebyshev-center based optimization method for targets localization. What we are most concerned with is the accuracy and performance of proposed algorithm. Thus, in this section, we firstly introduce the derivation CRLB and PCRLB for IMU/TOA fusion, and then to evaluate the fusion model's performance in both spatial and temporal aspects.

*Notations:*  $\nabla_a = [\frac{\partial}{\partial a_1}, \frac{\partial}{\partial a_2}, \dots, \frac{\partial}{\partial a_M}]^T$  denotes the gradient vector of  $a$ , and  $\Delta_b^a = \nabla_b \nabla_a^T$ .  $p(a)$  stands for the probability density function of the random variable  $a$ , and  $tr\{\cdot\}$  denotes the trace of the matrix.

### A. SPATIAL PERFORMANCE EVALUATION

#### 1) DERIVATION OF CRLB

CRLB is represented as a theoretical lower limit for any unbiased estimation and is widely used to assess localization performance. Thus, we comprehensively derive the CRLB for 2D localization of IMU/TOA fusion method in IoT to evaluate its spatial performance. Here come some definitions.

If  $\hat{\mathbf{m}}_k$  is an unbiased estimate of  $\mathbf{m}_k$ , then

$$E \left\{ (\hat{\mathbf{m}}_k - \mathbf{m}_k)^2 \right\} \geq CRLB = tr \left\{ J^{-1}(\mathbf{m}_k) \right\} \quad (30)$$

where  $J(\mathbf{m}_k)$  is the Fisher information matrix [41]. Before solving the Fisher information matrix, we need to first define the joint probability density function as

$$\begin{aligned} p(\hat{d}_k, \hat{l}_k, \hat{\theta}_k, \hat{\mathbf{m}}_k) \\ = \left\{ \prod_{n=1}^N p(\hat{d}_{n,k} | \mathbf{m}_k) \right\} p(\hat{l}_k | \mathbf{m}_{k-1}, \mathbf{m}_k) p(\hat{\theta}_k | \mathbf{m}_{k-1}, \mathbf{m}_k) \end{aligned} \quad (31)$$

where  $p(\hat{l}_k | \mathbf{m}_{k-1}, \mathbf{m}_k)$ ,  $p(\hat{\theta}_k | \mathbf{m}_{k-1}, \mathbf{m}_k)$  and  $p(\hat{d}_{n,k} | \mathbf{m}_k)$  can be obtained according to equations (2)~(7).

According to the joint probability density function, we can define the Fisher information matrix as

$$J(\mathbf{m}_k)_{i,j} = -E \left[ \frac{\partial^2 \ln p(\hat{d}_k, \hat{l}_k, \hat{\theta}_k, \hat{\mathbf{m}}_k)}{\partial \mathbf{m}_{k,i} \partial \mathbf{m}_{k,j}} \right], \quad i, j = 1, 2. \quad (32)$$

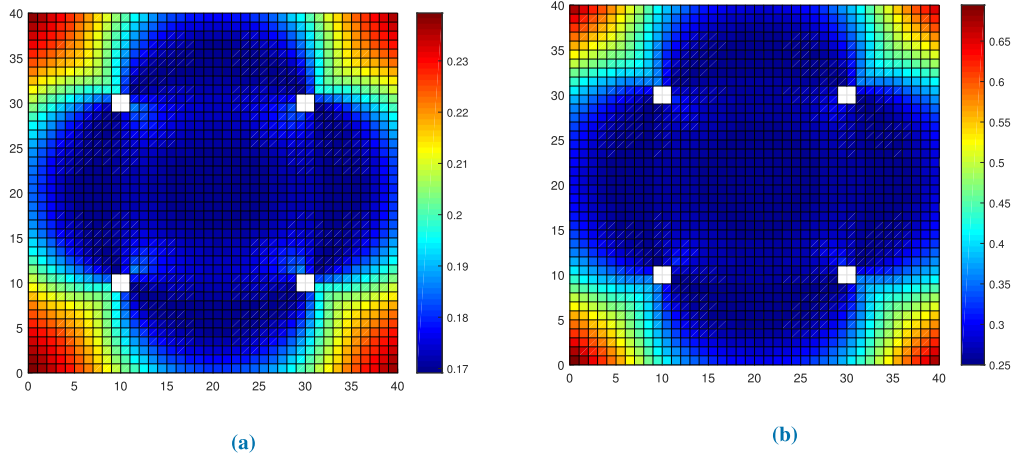


**FIGURE 2.** Spatial performance evaluation based on the analysis of CRLB. (a) CRLB simulation result based on the method of IMU/TOA fusion, whose maximum error is below 0.24m. (b) CRLB simulation result based on the method of sole TOA, whose maximum error is around 0.7.

Bringing Equation (31) into Equation (32) can calculate each element of the Fisher Information Matrix, and further obtain CRLB.

## 2) SIMULATION VERIFICATION

In this chapter, we intend to verify above derived CRLB for IMU/TOA fusion, and to prove that it is feasible to improve the positioning accuracy by the fusion of IMU and TOA.

We set up a  $40m \times 40m$  squared test-field for simulation. Four anchor nodes are deployed in the scene and distributed in the corners, whose coordinates are respectively (10,10), (10,30), (30,10), (30,30). Target nodes are randomly distributed in this test-field. For brevity, we assume that the communication range of the anchor nodes can cover the entire area, and all required information could be received from target nodes.

Fig. 2 shows the CRLB simulation result of proposed IMU/TOA fusion method (i.e., Fig. 2-(a)), as well as that when only TOA is applied (i.e., Fig. 2-(b)), under given measurement variances ( $\sigma_{1,k}^2 = 0.5 m^2$ ,  $\sigma_{2,k}^2 = 10^\circ$ ,  $\sigma_{3,k}^2 = 0.5 m^2$ ). Following conclusions could be drawn:

- 1) When proposed IMU/TOA fusion method is applied, the lower bound of localization system in this scenario is around 0.23m, while that of only TOA method is around 0.65m. An improvement of about 0.42m could be achieved.
- 2) In certain scenario, the best localization accuracy (measurement variance) could reach 0.17m, while that of only TOA method is around 0.25m. The fusion method is proved to have a better precision performance.

It is worth to mention that CRLB, when only IMU is applied, is not presented, as CRLB is a kind of performance indicator about spatial accuracy. However, the tracking result of IMU is obtained by continuous integration, that is, it is a time-related method. Thus, CRLB is not suitable for judging its performance. In next chapter, we will discuss about

PCRLB, which is based on temporal analysis, to evaluate the performance of IMU.

## B. TEMPORAL PERFORMANCE EVALUATION

### 1) DERIVATION OF PCRLB

Sequential tracking is supposed to be a temporal problem other than a sole spatial one. These continuous information could be used to evaluate the performance of given algorithms. Thus, we extend above CRLB to PCRLB with considering posterior information.

Before the derivation, we redefine the joint probability density function as

$$\begin{aligned} p(\hat{d}_k, \hat{l}_k, \hat{\theta}_k, \hat{\mathbf{m}}_k) \\ = p(\hat{d}_0 | \mathbf{m}_0) \prod_{k=1}^K p(\hat{l}_k | \mathbf{m}_{k-1}, \mathbf{m}_k) p(\hat{\theta}_k | \mathbf{m}_{k-1}, \mathbf{m}_k) p(\hat{d}_k | \mathbf{m}_k) \end{aligned} \quad (33)$$

To calculate the Fisher information matrix at state  $k$ , we define

$$p_k = p(\hat{d}_{0:k}, \hat{l}_{0:k}, \hat{\theta}_{0:k}, \hat{\mathbf{m}}_{0:k}) \quad (34)$$

where  $\hat{d}_{0:k}$ ,  $\hat{l}_{0:k}$ ,  $\hat{\theta}_{0:k}$ ,  $\hat{\mathbf{m}}_{0:k}$  represent ranging distance, step length, horizontal angle and target coordinate vector from the start state to state  $k$ , respectively. Therefore,

$$\begin{aligned} J(\mathbf{m}_{0:k}) \\ = \begin{bmatrix} E\left\{-\Delta_{\mathbf{m}_{0:k-1}}^{m_{0:k-1}} lnp_k\right\} & E\left\{-\Delta_{\mathbf{m}_{0:k-1}}^{m_{0:k}} lnp_k\right\} \\ E\left\{-\Delta_{\mathbf{m}_{0:k}}^{m_{0:k-1}} lnp_k\right\} & E\left\{-\Delta_{\mathbf{m}_{0:k}}^{m_{0:k}} lnp_k\right\} \end{bmatrix} \\ = \begin{bmatrix} \mathbf{A}_k & \mathbf{B}_k \\ \mathbf{B}_k^T & \mathbf{C}_k \end{bmatrix} \end{aligned} \quad (35)$$

According to [47], the sub-matrix  $J_k$  can be obtained by pseudo-inverse of the matrix  $J(\mathbf{m}_{0:k})$ , i.e.,

$$J_k = \mathbf{C}_k - \mathbf{B}_k^T \mathbf{A}_k^{-1} \mathbf{B}_k \quad (36)$$

According to equations (33) and (34), the joint probability density for the  $k + 1$  state is

$$p_{k+1} = p_k p(\hat{l}_{k+1} | \mathbf{m}_k, \mathbf{m}_{k+1}) p(\hat{\theta}_{k+1} | \mathbf{m}_k, \mathbf{m}_{k+1}) \\ p(\hat{d}_{k+1} | \mathbf{m}_{k+1}) \quad (37)$$

According to the joint probability density of state  $k + 1$ , we can find that

$$J(\mathbf{m}_{0:k+1}) = \begin{bmatrix} \mathbf{A}_k & \mathbf{B}_k & 0 \\ \mathbf{B}_k^T & \mathbf{C}_k + \mathbf{H}_k^{11} & \mathbf{H}_k^{12} \\ 0 & \mathbf{H}_k^{12} & \beta_{k+1} + \mathbf{H}_k^{22} \end{bmatrix} \quad (38)$$

where  $\mathbf{H}_k^{11}$ ,  $\mathbf{H}_k^{12}$ ,  $\mathbf{H}_k^{22}$  reflect the posterior information from state  $k$  to state  $k + 1$ , namely

$$\mathbf{H}_k^{11} = E_{\hat{l}, \hat{\theta}} \{-\Delta_{\mathbf{m}_k}^{m_k} \ln p(\hat{l}_{k+1} | \mathbf{m}_k, \mathbf{m}_{k+1}) p(\hat{\theta}_{k+1} | \mathbf{m}_k, \mathbf{m}_{k+1})\} \quad (39)$$

$$\mathbf{H}_k^{12} = E_{\hat{l}, \hat{\theta}} \{-\Delta_{\mathbf{m}_k}^{m_{k+1}} \ln p(\hat{l}_{k+1} | \mathbf{m}_k, \mathbf{m}_{k+1}) p(\hat{\theta}_{k+1} | \mathbf{m}_k, \mathbf{m}_{k+1})\} \\ = (\mathbf{H}_k^{12})^T \quad (40)$$

$$\mathbf{H}_k^{22} = E_{\hat{l}, \hat{\theta}} \{-\Delta_{\mathbf{m}_{k+1}}^{m_{k+1}} \ln p(\hat{l}_{k+1} | \mathbf{m}_k, \mathbf{m}_{k+1}) p(\hat{\theta}_{k+1} | \mathbf{m}_k, \mathbf{m}_{k+1})\} \quad (41)$$

$\beta_{k+1}$  reflects the location information based on TOA ranging [11], namely

$$\beta_{k+1} = E_{\hat{d}_{k+1}} \{-\Delta_{\mathbf{m}_{k+1}}^{m_{k+1}} \ln p(\hat{d}_{k+1} | \mathbf{m}_{k+1})\} \quad (42)$$

From  $J(\mathbf{m}_{0:k} : +1)$  and  $J_k$  we can get the Fisher information matrix for state  $k + 1$ , i.e.,

$$J_{k+1} = \beta_{k+1} + \mathbf{H}_k^{22} - [\mathbf{0} \ \mathbf{H}_k^{12}] \begin{bmatrix} \mathbf{A}_k & \mathbf{B}_k \\ \mathbf{B}_k^T & \mathbf{C}_k + \mathbf{H}_k^{11} \end{bmatrix} \begin{bmatrix} 0 \\ \mathbf{H}_k^{12} \end{bmatrix} \\ = \beta_{k+1} + \mathbf{H}_k^{22} - \mathbf{H}_k^{12} (J_k + \mathbf{H}_k^{11})^{-1} \mathbf{H}_k^{12} \quad (43)$$

Due to the step error and the directional error obey Gaussian distribution,  $\mathbf{H}_k^{11} = \mathbf{H}_k^{12} = \mathbf{H}_k^{22} = \mathbf{H}_k$  can be calculated. The solution of  $H_k$  can be referred to [36].

In summary, the posterior Fisher information matrix is

$$J_{k+1} = \beta_{k+1} + \mathbf{H}_k - \mathbf{H}_k (J_k + \mathbf{H}_k)^{-1} \mathbf{H}_k \quad (44)$$

According to the SMW (Sherman-Morrison-Woodbury) formula [46], it can be further simplified as

$$J_{k+1} = \beta_{k+1} + (\mathbf{H}_k^{-1} + J_k^{-1})^{-1} \quad (45)$$

where  $\beta_{k+1}$  reflects the information based on TOA,  $\mathbf{H}_k$  reflects information based on IMU.

## 2) EXPERIMENTAL VERIFICATION

We use the root mean square of PCRLB to evaluate the performance of proposed IMU/TOA fusion model. As PCRLB is theoretical and only up to the statistical characteristic, we conduct Monte Carlo experiments to obtain the statistical average under a larger number of simulation tests. The root mean square of the PCRLB can be represented by  $\frac{1}{L} \sum_{i=1}^L P_i^i$ , where  $P_i^i$  represents the PCRLB of the mobile node in state  $k$  in the  $i$ th Monte Carlo experiment, and  $L$  represents the total number of Monte Carlo experiments. In this paper,  $L$  is taken

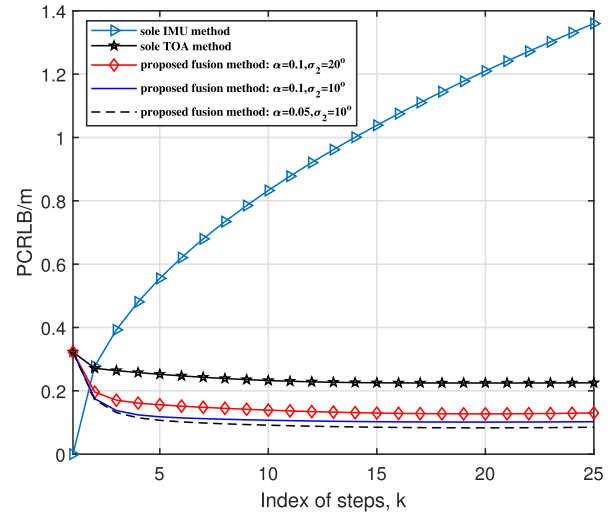


FIGURE 3. PCRLB of different positioning methods.

as 1000. Assume that the initial position of the mobile node is  $(1, 1)$ , and the mobile node performs random motion in the scene to ensure the equilibrium of entire target node's movement process.

Since TOA compensates for the accumulative error of the IMU during the entire motion, it is assumed that the step error and the directional error remain the same throughout the entire motion. The step error measured by the IMU is proportional to the actual step size, i.e.,  $\sigma_{1,k} = \eta l_k$ , where  $\eta$  is the proportional coefficient. Assume that  $\sigma_{2,k} = 10^\circ$ ,  $\sigma_{3,k} = 0.5m$ . Random motion is generated by Random Walk Model [48], and the sampling interval is 1s.

Fig. 3 shows the theoretical minimum error that can be achieved using sole TOA method, sole IMU method, and proposed IMU/TOA fusion method under 2-D test-field as mentioned. Following conclusions could be drawn:

- 1) When only IMU is adopted in the tracking system, the accumulative errors may tend to be diverging. Theoretically, this confirms that IMU based localization system faces the problem of accumulative errors. However, IMU/TOA fusion method can avoid this divergence. The performance curves of proposed approaches achieve stability after certain steps, i.e., their errors converge.
- 2) Compared with sole TOA tracking method, IMU/TOA fusion based method can significantly increase the accuracy (measurement variance) of human body motion tracking. The lower bound of proposed fusion method could drop below 0.1 m.

## C. COMPUTATIONAL COMPLEXITY EVALUATION

In the global convex estimation, a sensor only needs to broadcast the necessary information once. The information that sensor  $i$  broadcasts to its neighbors is  $\{d_{ij}, \bar{d}_{ij}, d_{ik}, \bar{d}_{ik}\}$ ,  $\forall j \in L_t, \forall k \in L_a$ . Therefore, the communication cost for sensor  $i$  is  $4m||L_{it} + L_{ia}||$ , where  $L_{it}$  denotes the number of

**TABLE 1.** The statistical root mean squared error (RMSE) and average CPU time obtained in the simulation experiment.

Numbers of Mobile Targets	RMSE (m)			CPU Time (s)		
	SQP	Active-set	Proposed method	SQP	Active-set	Proposed method
10	0.42	0.39	0.28	0.18	0.20	0.23
20	0.43	0.41	0.26	0.23	0.24	0.28
50	0.45	0.41	0.28	0.25	0.28	0.34
100	0.44	0.38	0.27	0.36	0.31	0.45

sensor  $i$ 's neighboring target nodes and  $L_{ia}$  denotes the number of sensor  $i$ 's neighboring anchor nodes. The computational cost comes from the SDP problem in (24), in which there are  $2L_t + 2L_a + N(2N + 1) + 1$  scalar variables to be optimized, and the number of scalar equality/inequality constraints is  $M + 2L_t + 2L_a$ . In (24), the computational complexity of SDP used in CVX is  $O(N^6)$  [44], and the computational complexity of the matrix inverse operation is  $O(N^3)$ . Thus, we can conclude that the computational complexity of our estimation algorithm is  $O(N^6)$ .

To further verify the computational performance, we implemented proposed method and compared it with state-of-the-arts, namely SQP [20] and Active-set [34]. We set up a simulation test-field with four base stations (Anchors) whose coordinates are respectively  $(0, 0)$ ,  $(100, 0)$ ,  $(100, 100)$  and  $(0, 100)$ . Mobile sensors (Tag) are randomly and evenly distributed in the given scene. Initial abscissa and ordinate of each node are randomly chosen between  $[0, 100]$ , and 100 Monte Carlo trails are performed on an embedded platform Intel Atom E3826 processor, with 1.46 GHz clock speed [50], under the mean error of  $0.3\text{ m}$  and variance of  $1\text{ m}^2$ .

When different number of mobile targets are deployed in the experimental area, the statistical root mean squared error (RMSE) and average CPU time in seconds of proposed and comparative algorithms are obtained in simulation tests. The average CPU time can be represented by  $\frac{1}{C} \sum_{i=1}^C T_i$ , where  $T_i$  represents the CPU time of the mobile node in the  $i$ th Monte Carlo experiment, and  $C$  represents the total number of Monte Carlo experiments ( $C = 100$  is used in this paper).

It can be seen from Table 1 that when the number of mobile sensor nodes range from 10 to 100, the min-max algorithm based on the Chebyshev-center described in this paper, has obvious performance advantages and maintains the optimal estimation accuracy. It can be seen from the results of 100 Monte Carlo trials, the average CPU time, namely computational complexity of proposed method is slightly higher than those of SQP and Active-set, while they are still of the same order.

Above all, compared with comparative algorithms, the method described in this paper has acceptable time consumption with a relative higher localization accuracy.

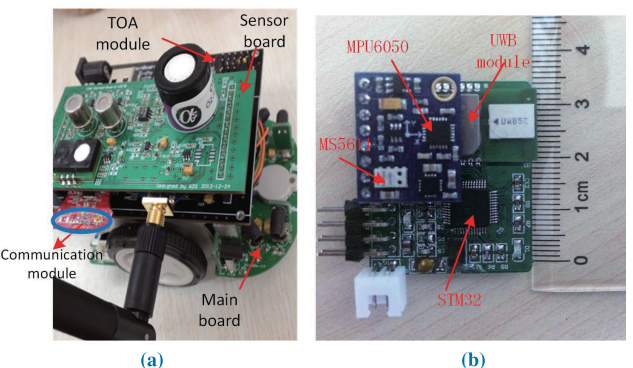


**FIGURE 4.** Experimental Platform Settings. (a) The wheeled navigation robot adopted in this paper. (b) A minimized sensor board specially designed for targets localization.

## V. PRACTICAL USE CASES

We propose an IMU/TOA fusion method for target tracking applications, introducing distance information into inertial systems. Based on above considerations, multi-targets localization experiments in both 2D navigation robots and 3D human motion tracking applications are carried out for verification, in order to better demonstrate the performance of proposed method when it is compared with state-of-the-arts.

## A. PLATFORM OVERVIEW AND EXPERIMENT SETUP

The wheeled navigation robot adopted in 2D tracking applications, as shown in Fig. 4-(a), has modular structure, mainly including the main board (provides a variety of interfaces, easy to expand), the core board (processor cortex-m4 STM32F405RG + 802.15.4 standard RF chip Atmel At86rf231), sensor board (integrated with a variety of sensors, including IMU and TOA module). The core board is connected with other equipment through the main board, so that the system can be disassembled and expanded.

A minimized sensor board is specially designed, as shown in Fig. 4-(b). It is aiming to collect spatial and temporal information during the motion process. Target data covers accelerated velocity, angular velocity and the distances between anchors and tags. Among these all, distance information

is especially special when compared with other platforms. Each sensor board has a 6-axes sensor (MPU6050, which integrates a triaxial accelerometer and a triaxial gyroscope), a barometer sensor (MS5611) and a UWB-TOA ranging module (DWM1000). The MEMS sensors are connected to a micro-controller (STM32F103) for the sake of sampling efficiency in a rate of 10Hz.

The specially designed wearable sensor board was reused in 3D human motion tracking experiment. It is aiming to collect spatial and temporal information during the human motion process. Sensing nodes are designed and intended to be put on joints to capture the movement conditions. Target data covers acceleration and angular velocity, as well as the distances between moving target and fixed anchors.

### B. PRACTICAL USE CASE IN 2D SCENARIO

To verify proposed algorithm, an open filed covered  $40\text{ m} \times 40\text{ m}$  is chosen as a testing scenario, and practical experiments are conducted to compare proposed min-max optimization method based on Chebyshev-center with state-of-the-art methods. We deploy four base stations (Anchors) in a fixed square scene, whose coordinates are (10, 10), (10, 30), (30, 10) and (30, 30). Ten navigation robots are acted as localization targets (Tag), randomly and evenly distributed in the given scene. The navigation robots are programmed to travel periodically along the rectangular route in the area. We compare the overall error performance of proposed algorithm with state-of-the-arts to verify its effectiveness.

As shown in Fig. 5, an open filed covered  $40\text{ m} \times 40\text{ m}$  is chosen as a testing scenario. Three typical and state-of-the art algorithms are tested to show the advantages of our proposed method, namely

- 1) Only IMU is used for target tracking, when algorithm [39] is applied. For simplicity, we denote it as “IMU” method.
- 2) Only TOA is used for target tracking, when algorithm [51] is applied. For simplicity, we denote it as “LS” method.
- 3) Kalman based IMU/TOA fusion method displayed in literature [43] is applied. UWB based TOA tag nodes are mounted to the navigation robots and communicate with external anchor nodes, implementing Kalman filtering fusion algorithm. For simplicity and in order to separate it from our proposed method, we denote it as “Kalman filtering” method.

The navigation robots are programmed to travel periodically along the rectangular route in the area, which is drawn as solid black line in Fig. 5. Sampled data are transmitted to control unit. Experiment results of the three mentioned algorithms are drawn respectively in Fig. 5 and Fig. 6, from which we can conclude that:

- 1) When only IMU is used in the tracking process, the trajectory deviated severely with time, which is an inherent disadvantage of IMU. This also verifies the accumulated error and drift problem of IMU. The CDF curve shown in Fig. 6 also indicates that this

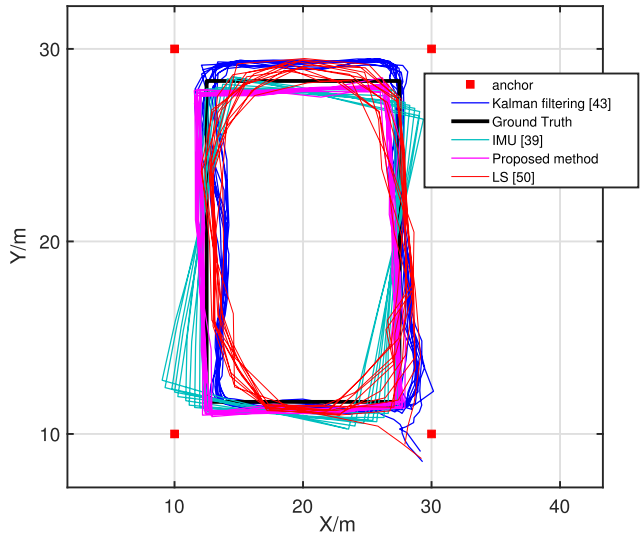


**FIGURE 5.** Walking trajectories of 2D tracking when proposed method and comparative algorithms are applied.

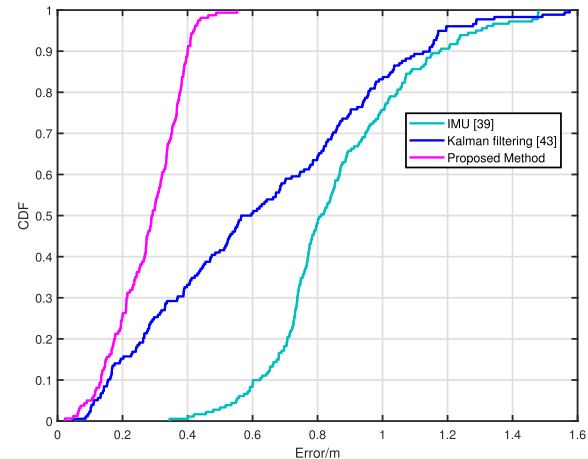


**FIGURE 6.** The accumulative distribution function (CDF) curve in 2D scenario when algorithms are applied.

method has the worst performance in 2D tracking scenario among all the three algorithms.

- 2) When only TOA measurements is used in the tracking process, it can be seen that the localization error is obviously higher than the method described in this paper, and the trajectory of LS is not as smooth as that of proposed method. It may be due to the following reasons: (1) LS is based on the assumption of small error regions, which generally cannot be satisfied in practical applications. It cannot be guaranteed that each measurement is small. (2) IMU and TOA fusion is realized by Kalman filtering [43]. Compared with LS [51], KF fusion method apparently has better accuracy, from which we can see the contribution of IMU measurements. (3) IMU has high instantaneous accuracy and a much higher sampling rate compared with TOA. The trajectory could be very smooth when IMU information

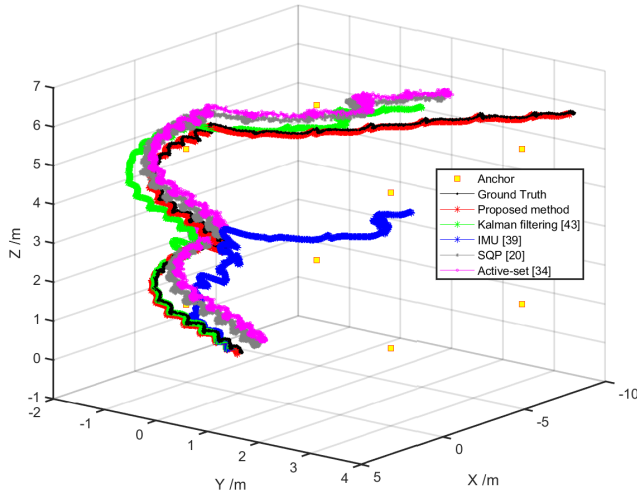


**FIGURE 7.** Walking trajectory when climbing spiral-stairs with our proposed method and four comparative methods.

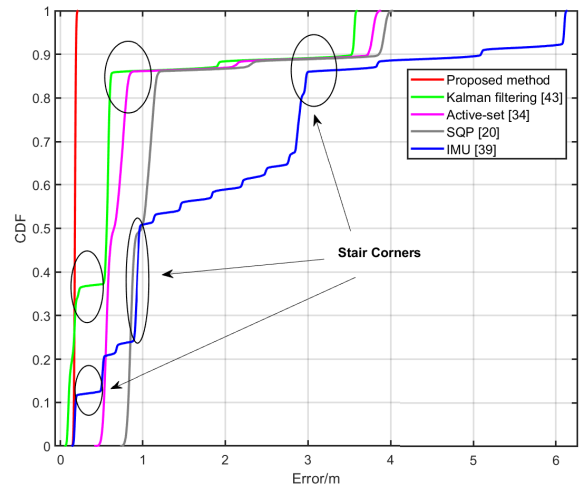


**FIGURE 8.** The accumulative distribution function (CDF) curve in 3D scenario when algorithms are applied.

is considered, as shown in Fig. 5. Thus, we could draw the conclusion that the IMU measurements contribute to the high tracking accuracy of proposed method and help better smooth the tracking trajectory.

- 3) IMU/TOA fusion method in [43] presents better performance, compared with that when only IMU or TOA is used. As the relative distance information measured by TOA is utilized, the error deviation problem is corrected to some extent when IMU/TOA method in [43] is used. The CDF curve in Fig. 6 also shows smaller errors and better performance.
- 4) As shown in Fig. 5 and Fig. 6, proposed method significantly decreases the drift errors and has lower tracking error (<0.6m), compared with that of 1.6 m when using Kalman-filtering based fusion method in [43]. It shows that among all the algorithms tested in our experiment, proposed method has the best tracking accuracy and can decrease drift errors to the maximum extent.

#### C. PRACTICAL USE CASE IN 3D SCENARIO

A spiral-stair (between two floors) scenario is selected as a 3D use case and four TOA anchors are located at each floor (totally eight anchors are used), as shown in Fig. 7. The location of anchors in each floor are referred to those in [43]. The experimenter was asked to walk up the stairs from 1st floor to 2nd and continue for some distance on the 2nd floor. A wearable sensor board as shown in Fig. 4-(b), was attached to the experimenter's right ankle.

In addition to above mentioned “IMU” and “Kalman filtering” comparative algorithms, two state-of-the-art optimization-based methods, i.e., SQP [20] and active-set [34], are also taken into consideration. For better comparison, ground truth and tracking trajectories with applying all mentioned methods (the proposed method and four comparative ones) are drawn in Fig. 7, from which following conclusions could be drawn:

- 1) With applying the proposed method, the experiment results are far closer to the ground truth, while on the other hand, the results when applying methods of “IMU” [39] and “Kalman filtering” [43] are drifting away as time accumulates. The result remains similar at the very beginning; however, the gap becomes larger while time goes on. Detailed accumulative errors are shown in Fig. 8.
- 2) Methods of using only IMU and “Kalman filtering” [43], both face the problem of drift error, especially when the experimenter turns around at stair corners, which can be indicated from Fig. 8. Time accumulated errors are more likely to be caused when moving direction changes. With “Kalman filtering” method applied into the algorithm, localization error to some extent can be fixed, but it still exists and it is also critical at turns. On the contrary, our proposed tracking method shows a good stability and no clearly drift errors are observed in our experiment.
- 3) Optimization-based approaches, i.e., SQP [20], Active-set [34] and our proposed method, do not face the problem of accumulative errors and drifting. However, SQP and Active-set show a certain overall error deviation during the whole tracking process. Besides, in some cases, e.g., at corners and edges of the experiment field, some large instantaneous errors are generated, which may be caused by its premature convergence (i.e., local optimization) during the solution process for optimization.

Based on above analysis, towards IMU/TOA fusion applications, our proposed method shows better performance when compared with state-of-art filtering methods, as well as optimization-based ones. With considering the real position of the target, our proposed Chebyshev-center-based optimization method does not face the problem of drift errors, but also

has significantly higher localization accuracy than state-of-the-art optimization methods.

## VI. CONCLUSIONS

This paper presents a min-max optimization method based on Chebyshev-center. Geometrically considering the real position of the target, it aims at improving the target tracking accuracy. Cramér-Rao lower bound (CRLB) and Posterior Cramér-Rao lower bound (PCRLB) for IMU/TOA fusion are derived to characterize both spatial and temporal localization performance of proposed fusion method. Simulation results show that proposed fusion method in this paper has obvious spatial-temporal performance advantages in theory. Practical use cases are also conducted, and experimental results show that proposed method significantly decreases the drift errors and has lower tracking error, compared with state-of-the-arts.

## ACKNOWLEDGMENT

(Cheng Xu and Jie He are co-first authors.)

## REFERENCES

- [1] L. Dong, W. Shu, G. Han, X. Li, and J. Wang, "A multi-step source localization method with narrowing velocity interval of cyber-physical systems in buildings," *IEEE Access*, vol. 5, pp. 20207–20219, 2017.
- [2] L. Lasmadi, A. Cahyadi, S. Herdjunanto, and R. Hidayat, "Inertial navigation for quadrotor using Kalman filter with drift compensation," *Int. J. Electr. Comput. Eng.*, vol. 7, no. 5, p. 2596, 2017.
- [3] B. Fasel, "Drift reduction for inertial sensor based orientation and position estimation in the presence of high dynamic variability during competitive skiing and daily-life walking," in *Proc. EPFL*, 2017, pp. 85–92.
- [4] A. Mosenia, S. Sur-Kolay, A. Raghunathan, and N. K. Jha, "Wearable medical sensor-based system design: A survey," *IEEE Trans. Multi-Scale Comput. Syst.*, vol. 3, no. 2, pp. 124–138, Apr./Jun. 2017.
- [5] C. Xu, J. He, X. Zhang, P.-H. Tseng, and S. Duan, "Toward near-ground localization: Modeling and applications for TOA ranging error," *IEEE Trans. Antennas Propag.*, vol. 65, no. 10, pp. 5658–5662, Oct. 2017.
- [6] R. Gravina, P. Alinia, H. Ghasemzadeh, and G. Fortino, "Multi-sensor fusion in body sensor networks: State-of-the-art and research challenges," *Inf. Fusion*, vol. 35, pp. 68–80, May 2017.
- [7] J. B. Zhang, P. Z. Zhang, and D. U. Kun-Kun, "Wireless sensor networks time synchronization based on GPS," *Transducer Microsyst. Technol.*, vol. 28, no. 6, pp. 31–33, 2009.
- [8] Y. Shen and M. Z. Win, "Fundamental limits of wideband localization—Part I: A general framework," *IEEE Trans. Inf. Theory*, vol. 56, no. 10, pp. 4956–4980, Oct. 2010.
- [9] N. Patwari, A. O. Hero, M. Perkins, N. S. Correal, and R. J. O'Dea, "Relative location estimation in wireless sensor networks," *IEEE Trans. Signal Process.*, vol. 51, no. 8, pp. 2137–2148, Aug. 2003.
- [10] S. Zhao, Y. S. Shmaliy, P. Shi, and C. K. Ahn, "Fusion Kalman/UFIR filter for state estimation with uncertain parameters and noise statistics," *IEEE Trans. Ind. Electron.*, vol. 64, no. 4, pp. 3075–3083, Apr. 2017.
- [11] D. Briese, H. Kunze, and G. Rose, "UWB localization using adaptive covariance Kalman filter based on sensor fusion," in *Proc. IEEE 17th Int. Conf. Ubiquitous Wireless Broadband (ICUWB)*, Sep. 2017, pp. 1–7.
- [12] H. Kim, B. Liu, C. Y. Goh, S. Lee, and H. Myung, "Robust vehicle localization using entropy-weighted particle filter-based data fusion of vertical and road intensity information for a large scale urban area," *IEEE Robot. Autom. Lett.*, vol. 2, no. 3, pp. 1518–1524, Jul. 2017.
- [13] Z. Liu, L. Zhang, Q. Liu, Y. Yin, L. Cheng, and R. Zimmermann, "Fusion of magnetic and visual sensors for indoor localization: Infrastructure-free and more effective," *IEEE Trans. Multimedia*, vol. 19, no. 4, pp. 874–888, Apr. 2017.
- [14] M. Miezal, B. Taetz, and G. Bleser, "On inertial body tracking in the presence of model calibration errors," *Sensors*, vol. 16, no. 7, p. 1132, 2016.
- [15] E. Jovanov et al., "A WBAN system for ambulatory monitoring of physical activity and health status: Applications and challenges," in *Proc. Int. Conf. Eng. Med. Biol. Soc.*, 2005, p. 3810.
- [16] R. Saeedi, J. Purath, K. Venkatasubramanian, and H. Ghasemzadeh, "Toward seamless wearable sensing: Automatic on-body sensor localization for physical activity monitoring," in *Proc. Conf. IEEE Eng. Med. Biol. Soc.*, Aug. 2014, pp. 5385–5388.
- [17] J. Liang, Y. Wang, and X. Zeng, "Robust ellipse fitting via half-quadratic and semidefinite relaxation optimization," *IEEE Trans. Image Process.*, vol. 24, no. 11, pp. 4276–4286, Nov. 2015.
- [18] P. A. Floor et al., "In-body to on-body ultrawideband propagation model derived from measurements in living animals," *IEEE J. Biomed. Health Inform.*, vol. 19, no. 3, pp. 938–948, May 2015.
- [19] J. C. Nascimento, M. Barão, J. S. Marques, and J. M. Lemos, "Information geometric algorithm for estimating switching probabilities in space-varying HMM," *IEEE Trans. Image Process.*, vol. 23, no. 12, pp. 5263–5273, Dec. 2014.
- [20] F. Bai, T. Vidal-Calleja, and S. Huang, "Robust incremental SLAM under constrained optimization formulation," *IEEE Robot. Autom. Lett.*, vol. 3, no. 2, pp. 1207–1214, Apr. 2018.
- [21] Y. Zhang and Y. L. Zhu Shen, "A semidefinite relaxation approach to positioning in hybrid sensor networks," in *Proc. IEEE 83rd Veh. Technol. Conf.*, May 2016, pp. 1–5.
- [22] Z. Cai, X. Yang, and X. Wu, "Tetrahedron-constraint least square localization algorithm in mixed LOS/NLOS scenario based on TDOA measurements," in *Proc. Int. Symp. Comput., Consum. Control*, Jul. 2016, pp. 251–255.
- [23] V. Bonnet, C. Mazzà, P. Fraisse, and A. Cappozzo, "A least-squares identification algorithm for estimating squat exercise mechanics using a single inertial measurement unit," *J. Biomech.*, vol. 45, no. 8, pp. 1472–1477, 2012.
- [24] B. Fasel, J. Spörri, J. Chardonnens, J. Kröll, E. Müller, and K. Aminian, "Joint inertial sensor orientation drift reduction for highly dynamic movements," *IEEE J. Biomed. Health Inform.*, vol. 22, no. 1, pp. 77–86, Jan. 2018.
- [25] H. Wyneersch, J. Lien, and M. Z. Win, "Cooperative localization in wireless networks," *Proc. IEEE*, vol. 97, no. 2, pp. 427–450, Feb. 2009.
- [26] I. Sharp, K. Yu, and Y. Guo, "GDOP analysis for positioning system design," *IEEE Trans. Veh. Technol.*, vol. 58, no. 7, pp. 3371–3382, Sep. 2009.
- [27] H. G. Aghamolki, Z. Miao, and L. Fan. (2018). "SOCP convex relaxation-based simultaneous state estimation and bad data identification." [Online]. Available: <https://arxiv.org/abs/1804.05130>
- [28] A. Domahidi, E. Chu, and S. Boyd, "Boyd ECOS: An SOCP solver for embedded systems," in *Proc. Eur. Control Conf.*, 2013, pp. 3071–3076.
- [29] P. Christoffersen and K. Jacobs, "The importance of the loss function in option valuation," *J. Financial Econ.*, vol. 72, no. 2, pp. 291–318, 2004.
- [30] E. Almazrouei, N. Al Sindi, S. R. Al-Araji, N. Ali, Z. Chaloupka, and J. Aweya, "Measurements and characterizations of spatial and temporal TOA based ranging for indoor WLAN channels," in *Proc. Int. Conf. Signal Process. Commun. Syst.*, 2013, pp. 1–7.
- [31] P.-H. Tseng and K. T. Feng, "Derivation of CRLB for linear least square estimator in wireless location systems," *Wireless Netw.*, vol. 18, no. 7, pp. 735–747, 2012.
- [32] H. A. Shaban, M. A. El-Nasr, R. M. Buehrer, "Toward a highly accurate ambulatory system for clinical gait analysis via UWB radios," *IEEE Trans. Inf. Technol. Biomed.*, vol. 14, no. 2, pp. 284–291, Mar. 2010.
- [33] Y. Zhang, Y. Zhu, and L. Shen, "A semidefinite relaxation approach to positioning in hybrid sensor networks," in *Proc. IEEE 83rd Veh. Technol. Conf.*, Nanjing, China, May 2016, pp. 1–5.
- [34] P. S. J. Sebastián, T. Virtanen, V. M. Garcia-Molla, and A. M. Vidal, "Analysis of an efficient parallel implementation of active-set Newton algorithm," *J. Supercomput.*, pp. 1–12, May 2018.
- [35] Z. He, Y. Ma, and R. Tafazolli, "Posterior Cramer-Rao bound for inertial sensors enhanced mobile positioning under the random walk motion model," *IEEE Wireless Commun. Lett.*, vol. 1, no. 6, pp. 629–632, Dec. 2012.
- [36] Y. Geng and K. Pahlavan, "Design, implementation, and fundamental limits of image and RF based wireless capsule endoscopy hybrid localization," *IEEE Trans. Mobile Comput.*, vol. 15, no. 8, pp. 1951–1964, Aug. 2016.
- [37] *Chebyshev Center*. Accessed: Jan. 11, 2019. [Online]. Available: <https://en.wikipedia.org>
- [38] G. Qin and X. W. G. Li, "Compensation method of magnetic field error of three dimensional vector based on ellipsoid compensation," *Electron. Meas. Technol.*, pp. 35–36, Jun. 2018.

- [39] J.-O. Nilsson, A. K. Gupta, and P. Händel, "Foot-mounted inertial navigation made easy," in *Proc. Int. Conf. Indoor Positioning Indoor Navigat.*, Oct. 2014, pp. 24–29.
- [40] X. *et al.*, "Robust localization using range measurements with unknown and bounded errors," *IEEE Trans. Wireless Commun.*, vol. 16, no. 6, pp. 4065–4078, Jun. 2017.
- [41] *Fmincon*. Accessed: Jan. 11, 2019. [Online]. Available: <https://baike.baidu.com/item/fmincon/17032570>
- [42] *CVX Toolbox*. Accessed: Jan. 11, 2019. [Online]. Available: <http://cvxr.com/cvx/>
- [43] S. Zihajehzadeh and E. J. Park, "A novel biomechanical model-aided imu/uwb fusion for magnetometer-free lower body motion capture," *IEEE Trans. Syst., Man, Cybern., Syst.*, vol. 47, no. 6, pp. 927–938, Jun. 2017.
- [44] S. Boyd and L. Vandenberghe, *Convex Optimization*. Cambridge, U.K.: Cambridge Univ. Press, 2004.
- [45] R. S. Chhikara and L. Folks, "*The Inverse Gaussian Distribution: Theory, Methodology, and Applications*". New York, NY, USA: Marcel Dekker, 1988, p. 259.
- [46] J. E. Guivant and E. M. Nebot, "Optimization of the simultaneous localization and map-building algorithm for real-time implementation," *IEEE Trans. Robot. Autom.*, vol. 17, no. 3, pp. 242–257, Jun. 2002.
- [47] P. Tichavsky, C. H. Muravchik, and A. Nehorai, "Posterior Cramer-Rao bounds for discrete-time nonlinear filtering," *IEEE Trans. Signal Process.*, vol. 46, no. 5, pp. 1386–1396, May 1998.
- [48] J. M. Pak, C. K. Ahn, Y. S. Shmaliy, P. Shi, and M. T. Lim, "Accurate and reliable human localization using composite particle/FIR filtering," *IEEE Trans. Human-Mach. Syst.*, vol. 47, no. 3, pp. 332–342, Jun. 2017.
- [49] A. De Angelis and C. Fischione, "Mobile node localization via Pareto optimization: Algorithm and fundamental performance limitations," *IEEE J. Sel. Areas Commun.*, vol. 33, no. 7, pp. 1288–1303, Jul. 2015.
- [50] *MinnowBoard*. Accessed: Jan. 11, 2019. [Online]. Available: <https://www.minnowboard.org/>
- [51] Y. T. Chan and K. C. Ho, "A simple and efficient estimator for hyperbolic location," *IEEE Trans. Signal Process.*, vol. 42, no. 8, pp. 1905–1915, Aug. 1994.



**CHENG XU** (S'17–M'19) received the B.E., M.S., and Ph.D. degrees from the University of Science and Technology Beijing, China, in 2012, 2015, and 2019, respectively, where he is currently with the Data and Cyber-Physical System Laboratory. His research interests include pattern recognition and the Internet of Things.



**JIE HE** received the B.E. and Ph.D. degrees in computer science from the University of Science and Technology Beijing, China, in 2005 and 2012, respectively, where he has been an Associate Professor with the School of Computer and Communication Engineering, since 2015. From 2011 to 2012, he was a Visiting Ph.D. Student with the Center for Wireless Information Network Studies, Worcester Polytechnic Institute. His research interests include wireless indoor positioning, human gesture recognition, and motion capture.



**YUANYUAN LI** is currently pursuing the master's degree with the University of Science and Technology Beijing. Her research interests include pattern recognition and the Internet of Things.



**XIAOTONG ZHANG** received the M.S. and Ph.D. degrees from the University of Science and Technology Beijing, in 1997 and 2000, respectively, where he is a Professor with School of Computer and Communication Engineering. His research interests include work in quality of wireless channels and networks, wireless sensor networks, networks management, cross-layer design and resource allocation of broadband and wireless networks, and signal processing of communication and computer architecture.



**XINGHANG ZHOU** is currently pursuing the bachelor's degree with the University of Science and Technology Beijing. His research interests include pattern recognition and the Internet of Things.



**SHIHONG DUAN** received the Ph.D. degree in computer science from the University of Science and Technology Beijing, where she is currently an Associate Professor with the School of Computer and Communication Engineering. Her research interests include wireless indoor positioning, human gesture recognition, and motion capture.